DANISH METEOROLOGICAL INSTITUTE

——— SCIENTIFIC REPORT———

00-14

Use of GPS observations in an optimum interpolation based data assimilation system

Bjarne Amstrup
Kristian S. Mogensen
Xiang-Yu Huang

DMI

COPENHAGEN 2000

Use of GPS observations in an optimum interpolation based data assimilation system

Bjarne Amstrup, Kristian S. Mogensen and Xiang-Yu Huang

Danish Meteorological Institute

Abstract

An Optimum Interpolation (OI) based data assimilation system is further developed to include geopotential profiles retrieved from Global Positioning System (GPS) occultation measurements. The error statistics of the profiles are estimated, and then used in the system. Important differences in the definition of geopotential height used in the GPS retrieval algorithm and that used in the Numerical Weather Prediction (NWP) models are addressed. An example of the impact on an analysis from the new data is also given.

The impact of the geopotential profiles retrieved from GPS/MET occultations on the data assimilation system is investigated. A 16-day period is chosen to run parallel experiments with or without the additional data included. Simple statistics are used to quantify the impact. The impact turns out to be neutral averaged over the whole period, but varies on daily basis.

1 Introduction

Atmospheric profiling using the radio occultation technique provides an additional data source for climate monitoring and numerical weather forecasting (see Høeg *et al.*, 1995 and references therein). As high quality conventional profile data are still inadequate for determining the three dimensional atmospheric state, especially over the oceans and in the southern hemisphere, the GPS profile data may become one of the most important future observing systems. Simulated occultation data have been assimilated into NWP models indicating a great potential of the new data (Eyre, 1994; Zou *et al.*, 1995).

In this study we intend to explore the possibility of using real data in an operational NWP system which is based on the OI analysis method. The real data are the retrieved geopotential profiles from the GPS/MET occultation measurements (Syndergaard *et al.*, 2000). The operational NWP system used in this study is the HIgh Resolution Limited-Area Modelling (HIRLAM) system implemented at the Danish Meteorological Institute (DMI) (Sass *et al.*, 1999).

Using the real data, one has to face and attack, among other things, the problems related to data error statistics. Quality control procedures are

1

necessary for removing erroneous data. Interpolation of the data in space is part of the OI scheme, but a strategy is needed for the interpolation in time. When using the operational NWP system, one has to keep the basic setup and only include the new component as a small addition. The impact of the new data could be small simply because they are few.

This report gives a brief overview of the DMI-HIRLAM (section 2), presents the approach we took in estimating the data error statistics (section 3), and shows an example of the impact from the new data on an analysis (section 5). Section 4 describes the observation system experiment (OSE) setup, section 6 defines the verification measures and section 7 gives some results from a few of the experiments.

2 DMI-HIRLAM

The data assimilation system used for the experiments is the operational HIRLAM forecasting system at DMI. The system has been developed in a collaborative research project between the national meteorological institutes of Denmark, Finland, France, Iceland, Ireland, the Netherlands, Norway, Spain, and Sweden (see e.g. Machenhauer, 1988; Gustafsson, 1993; Lynch *et al.*, 2000). It is an intermittent data assimilation system including an OI analysis scheme and a forecast model. The system at DMI is documented in Sass *et al.* (1999) and further details concerning the HIRLAM OI analysis scheme can be found in Källén (1996) and Undén (2000).

The HIRLAM OI is a limited area version of the ECMWF OI scheme (Lönnberg and Shaw, 1987). The first-guess field is the 6 h forecast based on the previous data assimilation cycle. Three-dimensional multi-variate statistical interpolation is used for the wind, geopotential, and surface pressure. Three-dimensional univariate statistical interpolation is used for relative humidity. The observation window covers a 6 h span around the time for the analysis (0000, 0600, 1200 and 1800 UTC). A standard observation set is used, including synoptic observations, ship observations, drifting and moored buoys, pilot balloons, radiosonde data and aircraft data. For radiosondes the OI system uses geopotential height, wind and humidity at a fixed number of pressure levels. Here we would like to point out that no satellite observations have been included except GPS profiles.

The GPS geopotential profiles have been included in the analysis scheme in the same way as for radiosondes, but with modified vertical correlations and observation errors. While the providers of GPS derived atmospheric profiles used WGS84 (World Geodetic System 1984) geometric heights, the geopotential heights widely used in NWP modeling are not referred to the WGS84 ellipsoid but to the EGM96 (Earth Gravitational Model 1996) geoid. Therefore, we made a conversion of WGS84 geometric heights to NWP model HIRLAM geopotential heights as described in Vedel (2000) .

2

3 Including GPS geopotential profiles

Optimum interpolation is also called statistical interpolation since the interpolation depends on knowledge of the statistical moments of the background and observation errors (see for example Daley, 1993). To include the GPS geopotential profiles, their error statistics in the form of an error covariance matrix are needed.

In the following $\langle\ \rangle$ denotes the average (or expectation value) of a large number of realizations of observations or pairs of observations. The bias is defined as the average value of the observations minus "true value" (denoted T here):

$$\text{bias}_k = \langle O_k - T_k \rangle$$

Here and in the following the subscripts k and l denote vertical levels. The standard deviation to be used for observation errors in the OI data assimilation scheme is calculated as:

$$\sigma_k = \sqrt{\langle (O_k - T_k - \text{bias}_k)^2 \rangle}$$

Finally the correlation is found by dividing the covariance by the two involved standard deviations:

$$R_{lk} = \frac{\langle (O_k - T_k - \text{bias}_k)(O_l - T_l - \text{bias}_l) \rangle}{\sigma_k \sigma_l}$$

averaging over the pairs of vertical levels.

For the GPS statistics, the error statistics and correlation have been calculated using ECMWF analyses or 3 hour forecasts when available and closer in time horizontally interpolated to the actual GPS measurements tangent point location. The interpolated values were then used as the "true value". This is probably the best estimate we can make for the *upper limit* of the retrieval errors since ECMWF analyses and forecasts contains errors, too, and the error estimate includes some background error. Furthermore, we have used all available GPS/MET-profiles in the period 2 - 16 Feb 1997, including the ones in the tropics and in the Southern Hemisphere.

A very simple quality control procedure is applied. If the "error" of a datum is larger than a critical value, the datum is considered as erroneous and excluded in the further applications. The results are sensitive to the choice of the critical value. Figure 1 shows bias and standard deviations used in the runs. When 200 m is used as the maximum height error allowed in the quality control, the standard deviation errors are more than twice the radiosonde height errors used in the OI analysis for pressure levels at and below 250 hPa. Therefore, the weights from GPS profiles are somewhat smaller than the corresponding weights for radiosonde observations. When 1000 m is used as the maximum height error allowed more data are accepted, but the standard deviation errors as well as the absolute value of bias errors

3

become larger, leading to smaller weights for the GPS geopotential data. The standard deviation increases by about 25 % at 300 hPa and 400 hPa, and by much more above 50 hPa and below 500 hPa. The number of samples used at the different pressure levels are typically reduced to about 40 % when reducing the error from 1000 m to 200 m in the quality control (see Figure 1 for the relevant numbers).

A typical example of the correlations for the levels used in the OI is shown in Figure 2. For this plot all GPS/MET profiles having "errors" less than 1000 m at all levels are used. The number of GPS/MET data used for the bias and standard deviation are less than half the numbers used for making the correlation values shown in Figure 2. It is seen that there is a very high degree of correlation as expected.

4 The OSE setup

A 16 day period, from 0000 UTC 1 Feb 1997 to 1800 UTC 16 Feb 1997, is chosen for the data assimilation experiment. This period allows for one day "spin-up" from the initial forecast starting from an ECMWF (European Centre for Medium-Range Weather Forecasts) analysis before the first GPS/MET profile on 2 Feb. The last GPS/MET profile from this period is on 16 Feb in the 1800 UTC data assimilation cycle. This period is also part of the FASTEX (Fronts and Atlantic Storm-Track EXperiment) period in which the radiosonde network was considerably enhanced over the North Atlantic area.

The data assimilation system used for the experiments is the operational HIRLAM forecasting system at DMI, documented in (Sass *et al.*, 1999), with two differences. One is the lateral boundaries. Instead of using the *available* ECMWF analyses and forecasts (which could be as old as a +60 h forecast) at the analysis time, we use the *best possible* ones, *i.e.* ECMWF analyses at 0000 UTC and 1200 UTC and +6 h forecasts at 0600 UTC and 1800 UTC. By doing this we hope to reduce problems due to old lateral boundaries (Gustafsson, 1990). Another difference is the forecast length at 0600 UTC and 1800 UTC. While in the operational DMI-HIRLAM-G setup only a +6 h forecast is scheduled at these times (made solely for data assimilation purposes), in both experiments a +48 h forecast is made after every analysis to expand the data samples and to regularize the verification statistics. In the parallel runs we used the largest of the present operational model domains (DMI-HIRLAM-G). This model domain is the one denoted "G" in Fig. 3. The horizontal resolution is 0.45°, the number of vertical levels is 31, the number of grid points is 202 × 190, the time step is 240 s, and the boundary update frequency is 1/(6 h).

A substantial number of different tests have been made with small changes, e.g., in the screening procedure. Here, we show results from 3 of the lat-
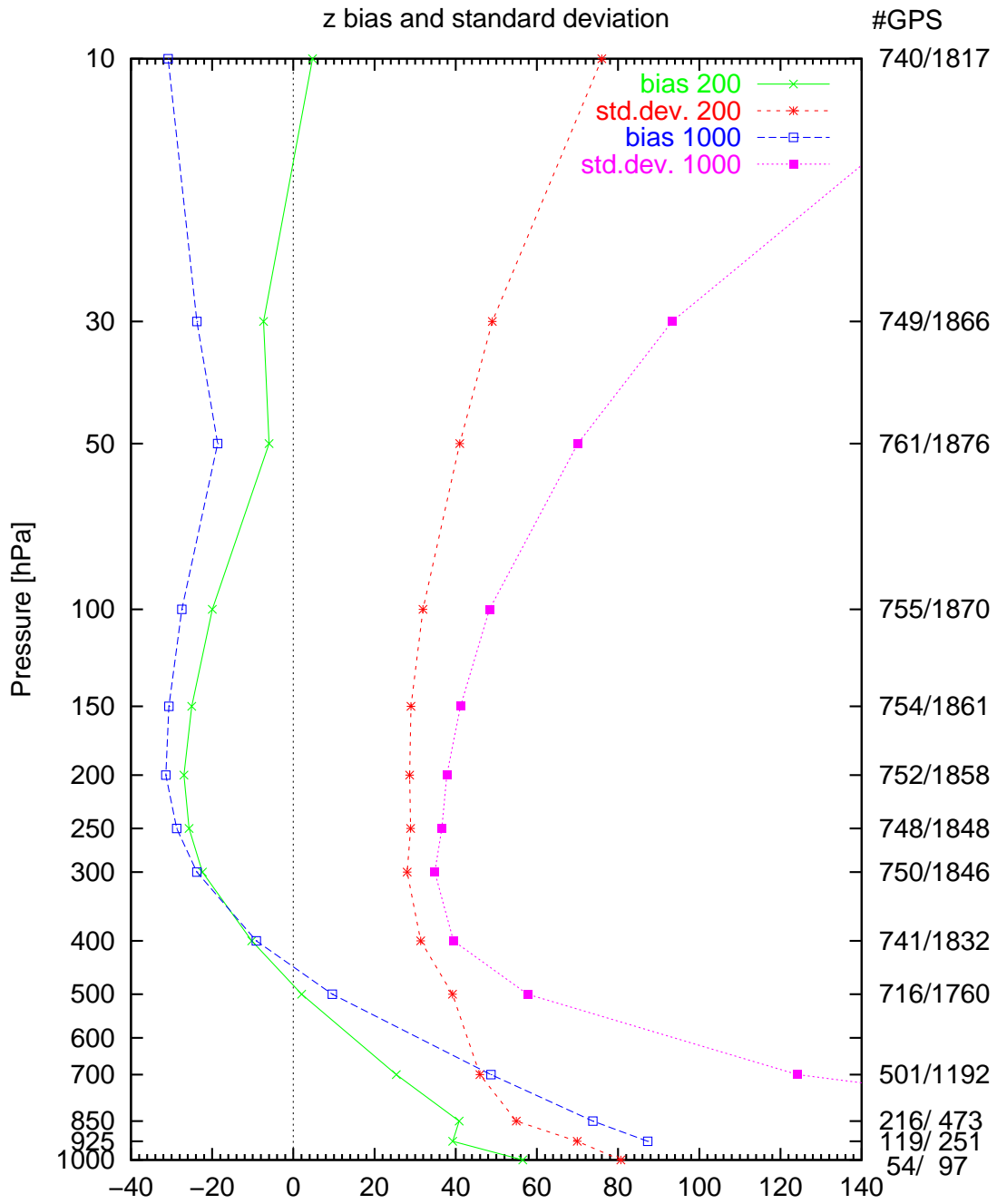
Figure 1: Bias and standard deviation (x-axis, in m) of geopotential height as a function of pressure (y-axis) for the levels used in the OI analysis. The number of GPS data (number of samples) used at each level is given on the right hand side. The smaller number is for the 200 m limit and the higher number is for the 1000 m limit.
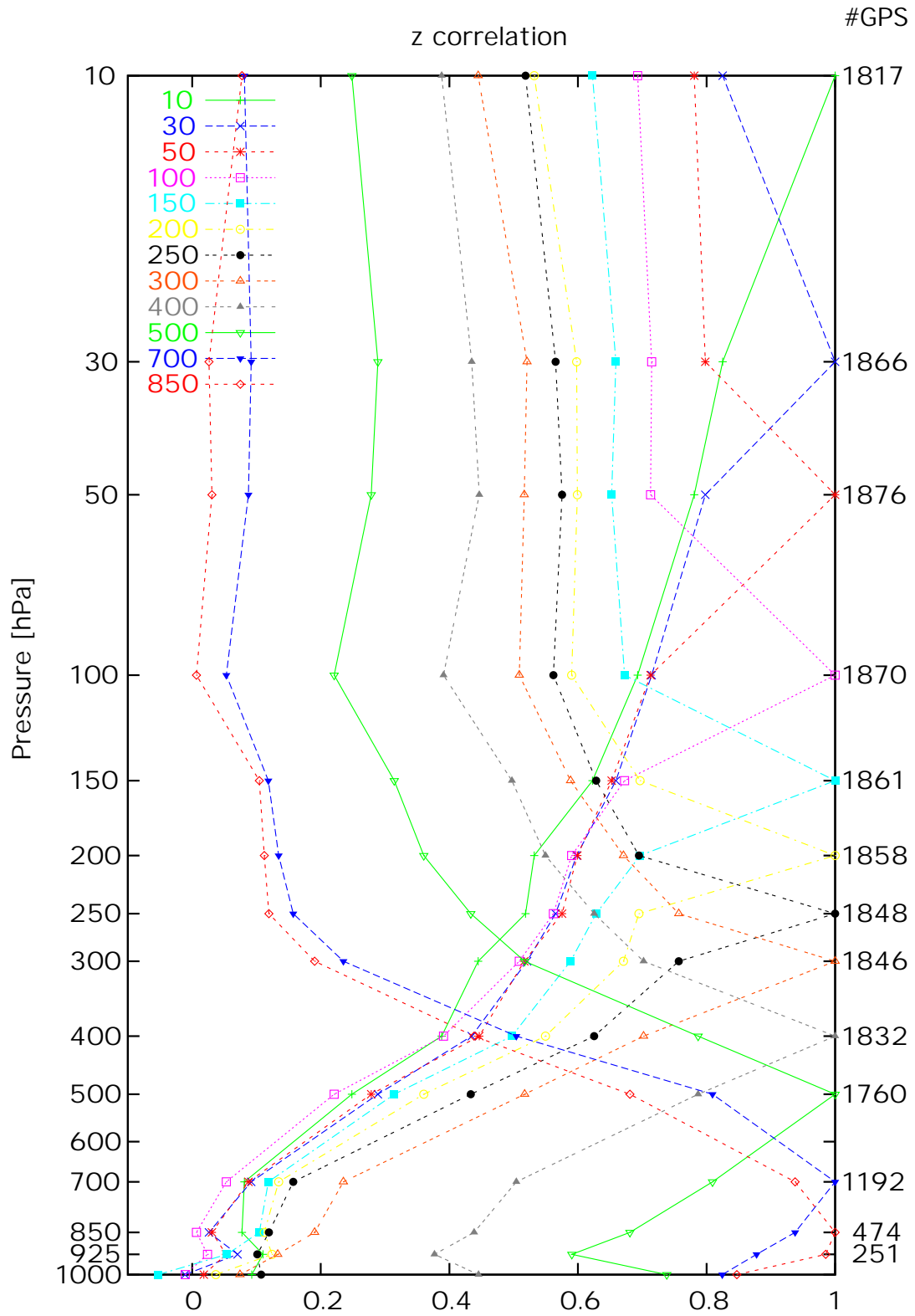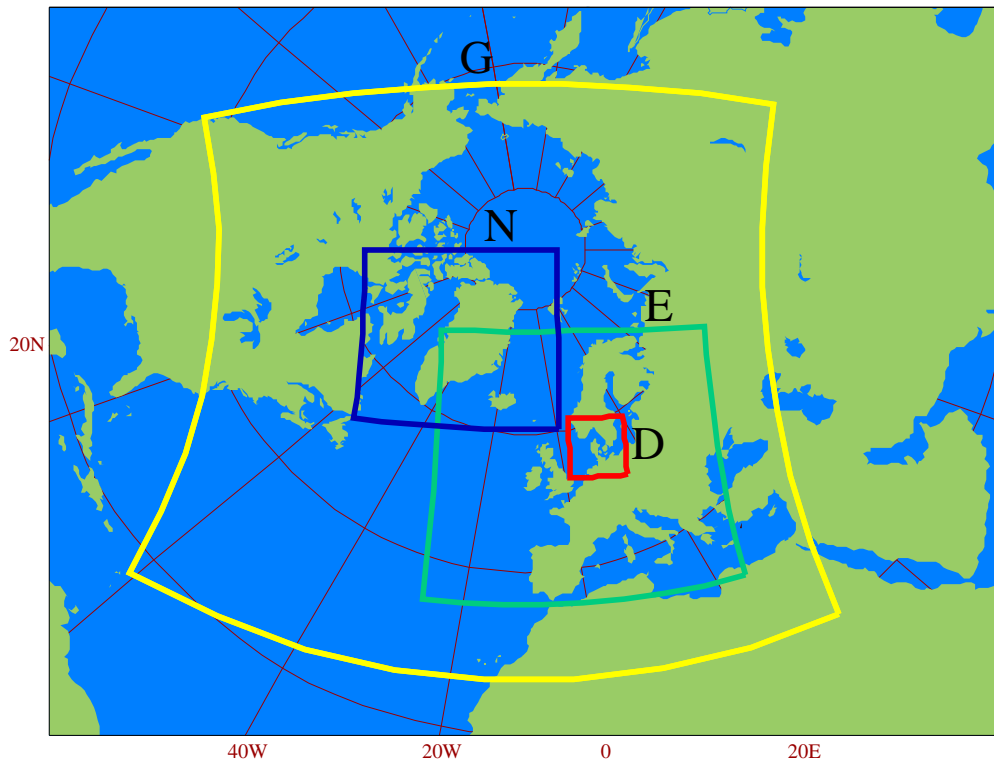
Figure 2: Mean vertical correlation (*x*-axis) of geopotential height as a function of pressure (*y*-axis) for the levels used in the OI analysis. The number of GPS data used at each level is given on the right hand side.

6

Figure 3: DMI operational model areas.

est runs. The experiment termed NOG is the control run with no GPS. The second experiment is named BIA using GPS/MET profiles that are bias-corrected so that the average geopotential height bias at a given pressure level has been removed. The last experiment is named WIG using GPS/MET profiles without the bias correction.

5 Impact on an analysis

Figure 4 shows difference plots of analyzed 300 hPa, 500 hPa and 850 hPa geopotential height fields from an analysis including 5 GPS/MET profiles and an analysis without these extra profiles. The first guess fields and other observation types were the same. The extra GPS/MET profiles may influence the analysis in two ways: either used as an extra information or by reducing the influence from other nearby observations of other types. The figure illustrates that the inclusion of GPS profiles give reasonable changes to the field. The profiles were located at the following positions defined by the position of the lowest tangent point: A (16.50°W,36.87°N), B (132.09°W,71.03°N), C (61.93°W,54.98°N), D (9.15°W,51.98°N), and E

(21.69°W,39.41°N).

Profile A is within 3° from a radiosonde. Profile B is in between two radiosondes, one of them is within 2.5°. Profile C at Ireland is almost collocated with a radiosonde in the same assimilation cycle. Despite this, they all have impact on the analysis. While the impact from profile A is mainly at higher levels, the impact from profiles B and C extends to lower levels.

Profiles D and E are over the ocean where profile-type data are really needed. Although profile D seems to "add" nothing to the analysis, profile E clearly has an impact from 500 hPa above.

The HIRLAM OI is a multi-variate analysis. Observations in geopotential also lead to analysis increments in wind through the cross-correlation of background errors. Figure 5 shows this impact of the GPS/MET profiles on wind analysis. The difference in wind analysis shows a cyclonic circulation around the positive height difference due to profile A and an anti-cyclonic circulation around the negative height differences due to profiles B, C and E. There are also differences caused by the imbalances due to the OI box structures, which may need further investigations.

6 Verification

The variables calculated in observation verification (obs-verification) are the standard ones: The mean deviation (bias), μ

$$\mu = \frac{1}{n_s} \sum_{i=1}^{n_s} \mathcal{E}_i,$$

the root-mean-square of the deviation, rms

$$\text{rms} = \sqrt{\frac{1}{n_s} \sum_{i=1}^{n_s} \mathcal{E}_i^2},$$

and the variance of the deviation, σ^2

$$\sigma^2 = \frac{1}{n_s} \sum_{i=1}^{n_s} \left(\mathcal{E}_i - \mu \right)^2, \tag{1}$$

where $\mathcal{E}_i$ is the deviation

$$\mathcal{E}_i = \left\{ \begin{array}{ccc} \phi_i^f - \phi_i^o & \text{for} & |\phi_i^a - \phi_i^o| \leq \epsilon, \\ 0 & \text{for} & |\phi_i^a - \phi_i^o| > \epsilon, \end{array} \right. \tag{2}$$

and n_s is the number of accepted samples in time and space i.e., the number of "i" that satisfy $|\phi_i^a - \phi_i^o| < \epsilon$, cf. equation (2). ϕ^f indicates the forecast and ϕ^o the observed value of some variable ϕ. ϕ^a indicates the computed
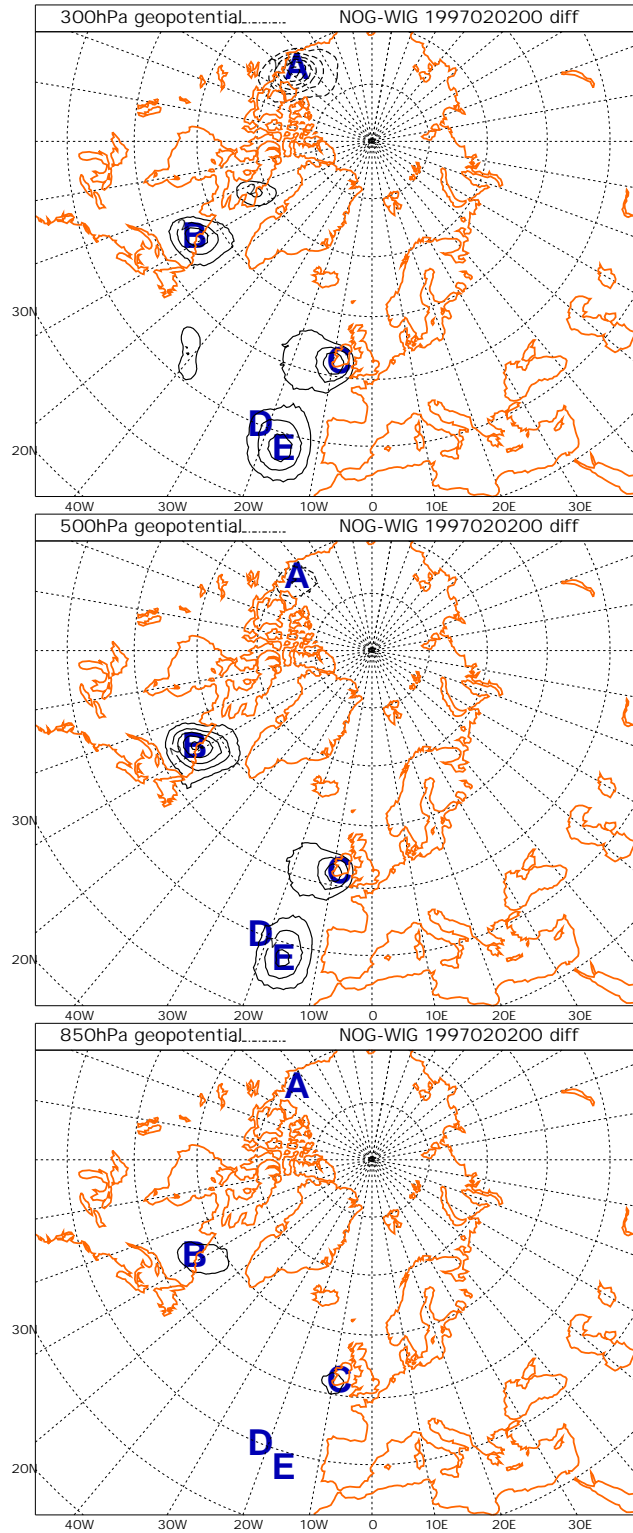
8

Figure 4: Difference plot of 850 hPa (lower), 500 hPa (middle) and 300 hPa (upper) geopotential height of an analysis including 5 GPS/MET-profiles and an analysis without GPS/MET profiles. The first guess field and other observations were identical. The approximate positions of the GPS/MET profiles are marked with blue capital letters. Contour lines are for every 1 m.
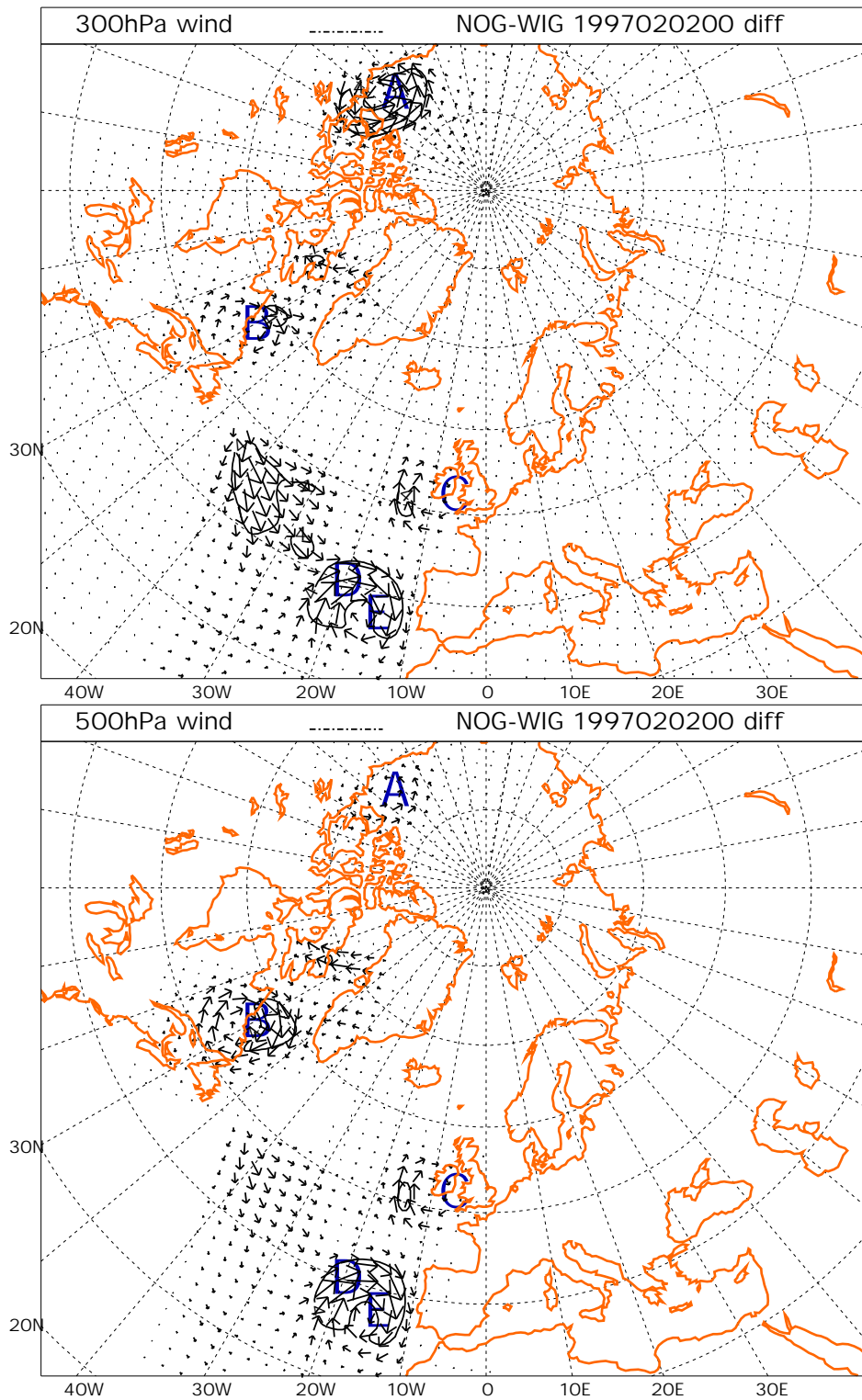
Figure 5: Difference plot of 300 hPa (upper) and 500 hPa (lower) wind of an analysis including 5 GPS/MET-profiles and an analysis without GPS/MET profiles. The first guess field and other observations were identical. The difference is multiplied by 10 and the length of the arrow indicates the length of the difference wind vector.
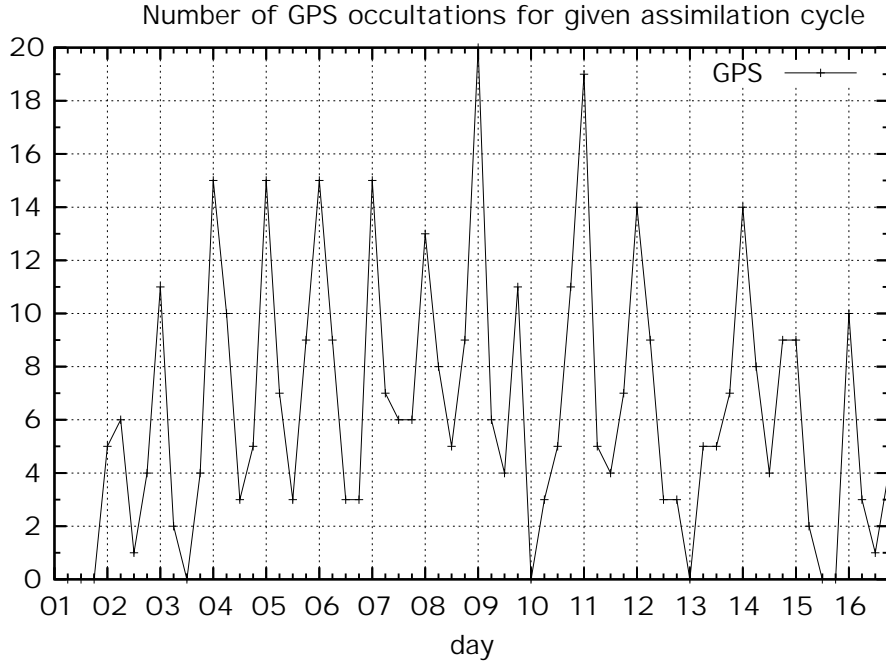
Figure 6: Number of GPS/MET profiles available for assimilation.

value of the analysis for the variable ϕ. Hence, if the difference between the observation value and the analysis value is too large, the observation value is rejected in the program. We use the standard EWGLAM values for the "allowed" differences.

Notice, that if the samples are independent random variables as assumed in the programs, the variance (1) can be computed using

$$\sigma^2 = \left(\frac{1}{n_s} \sum_{i=1}^{n_s} \mathcal{E}_i^2 \right) - \mu^2 \, . \tag{3}$$

The same methods, equations (1) and (3), are used on a grid-point by grid-point basis in field verification, except the deviation $\mathcal{E}_i$ is calculated as

$$\mathcal{E}_i = \phi_i^f - \phi_i^a \, , \tag{4}$$

where for ϕ^a ECMWF analyses are used.

7 Results from experiments

Figure 6 shows the number of GPS/MET profiles available within the model area for each cycle in the data assimilation experiments. There is a large variation from no profile to 20 profiles in one single assimilation cycle. On average, 6.7 profiles are available per assimilation cycle. Unfortunately, the largest numbers of GPS/MET profiles are in the 00 UTC data assimilation

11

cycles in which the numbers of radiosondes are also relatively large. The impact would potentially be larger if most of the profiles had been in the 06 UTC and 18 UTC data assimilation cycles where the numbers of radiosondes are relatively small. It should be noted that the extra FASTEX (Fronts and Atlantic Storm-Track EXperiment) radiosonde observations have been excluded in the first set of runs for which obs-verification is shown here. However, a similar set of experiments including these extra radiosonde observations show the same trends. Results from field verification is shown for a set of experiments including the FASTEX radiosonde observations.

Figure 7 shows obs-verification scores for the full period of mean sea level pressure (mslp), 850 hPa temperature, 500 hPa geopotential height, and 250 hPa wind speed. The differences in rms as well as bias scores are very small and the overall impact from GPS/MET profiles is neutral. Marginally positive impact is seen for forecast lengths around 24 to 30 hours and marginally negative impact is seen for 48 hours forecast except for mslp. The same trend is found (not shown) for other parameters.

When looking at daily verification scores an impact from the GPS/MET profiles can be seen. Figure 8 shows daily verification scores for 24 hours mslp forecasts, Figure 9 shows daily verification scores for 24 hours 850 hPa temperature forecasts, and Figure 10 shows daily verification scores for 24 hours 500 hPa geopotential height forecasts. For all these parameters there is a large daily variation and also differences in which one has the best score. Since the overall verification scores are neutral some GPS/MET profiles must have a positive impact and some a negative impact.

Figure 11 shows differences of standard deviation of 500 hPa geopotential height and mslp between a control run, NOG, and a run including GPS/MET data, WIG. It should be noted that it is the results from a second set of experiments different from the ones used for the obs-verification since no usable data were available for field verification from those experiments. Furthermore, the extra FASTEX radiosondes were included in these two runs. In some areas NOG is better and in other areas WIG is better when using these measures.

8 Conclusions

In this report, we have described a first assimilation of the geopotential profiles retrieved from the GPS/MET occultations with the DMI HIRLAM OI analysis and forecasting system.

We have modified the OI analysis to include GPS profiles similar to radiosonde profiles. A major work has been the estimation of the data error statistics. There are at least two limitations in our results: 1) error due to the selection of ECMWF analysis and forecast as "truth"; 2) representativeness due to the short period of available data. Re-estimations are necessary
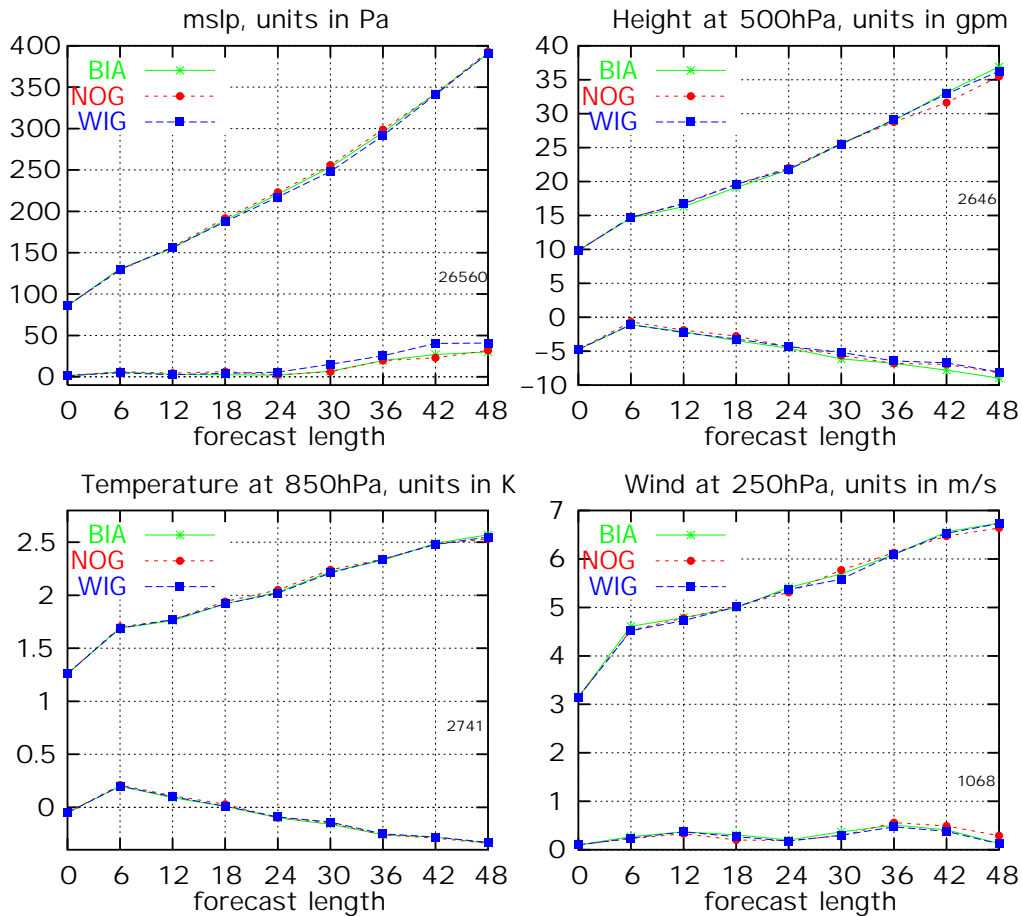
Figure 7: Obs-verification (bias and rms, extended EWGLAM station list) results of mslp (upper left), 850 hPa temperature (lower left), 500 hPa geopotential height (upper right), and 250 hPa wind speed (lower right). ECMWF analyses have been used to reject observations. The small number in the plot indicate the number of observations used in the verification.

whenever new data become available. Search for the "truth" or better estimates of it should continue. It should also be stressed that quality control plays an important role in the error statistics.

Although the GPS profiles are just a small addition to the existing observing systems used by the HIRLAM OI they are able to contribute significantly to the analysis increments. This is particularly true for the data sparse areas. These increments are likely to remain in the forecast due to the spatial correlations for both the background error and the observation error. The results show that the impact on forecasts are overall neutral, however, with significant daily variations.

Finally, it is still an open question which information from GPS occultation data should be assimilated into NWP models. In this study we have chosen the retrieved geopotentials, simply because the current HIRLAM OI
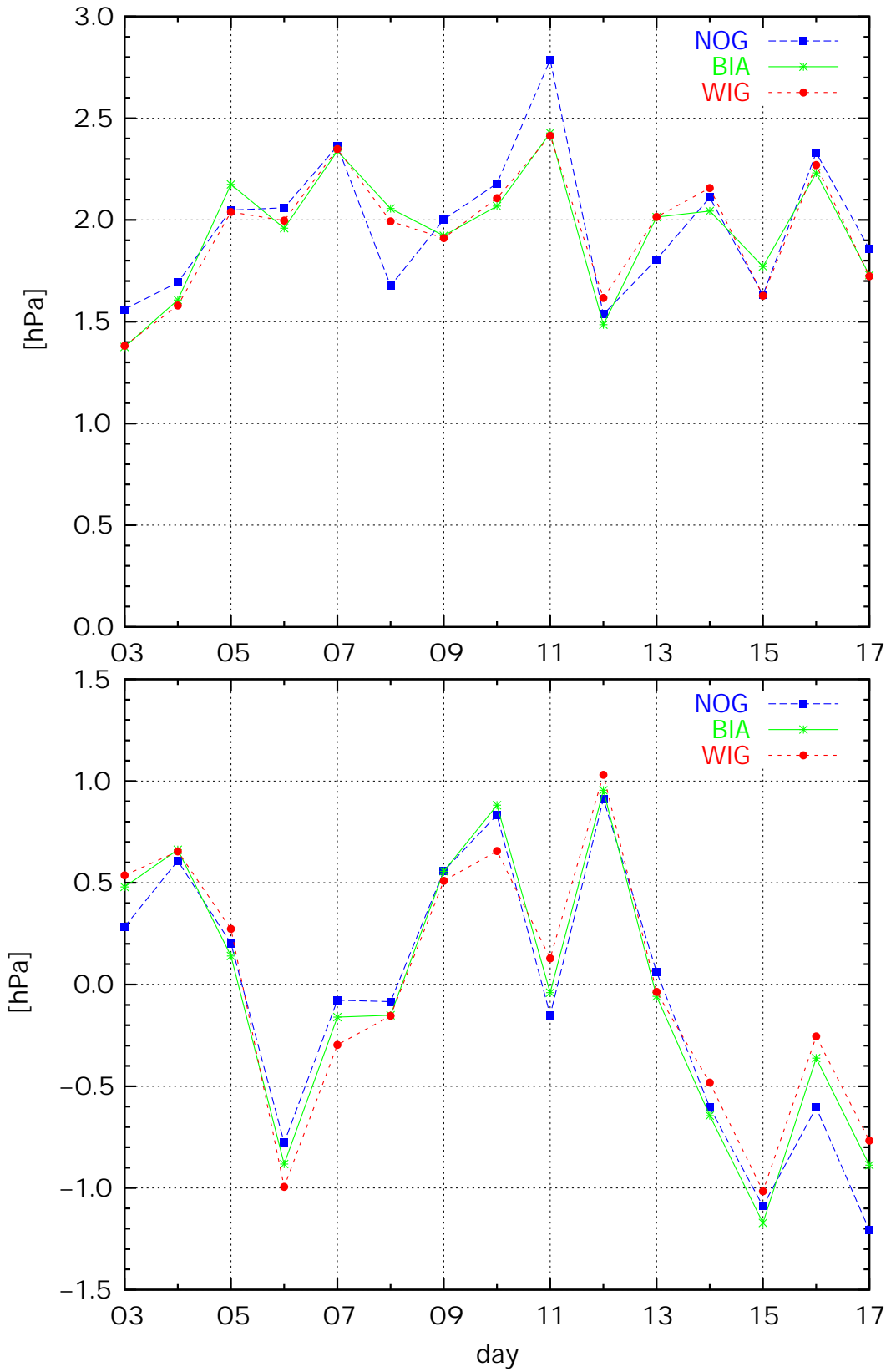
Figure 8: Daily obs-verification of 24 hours mslp forecast.
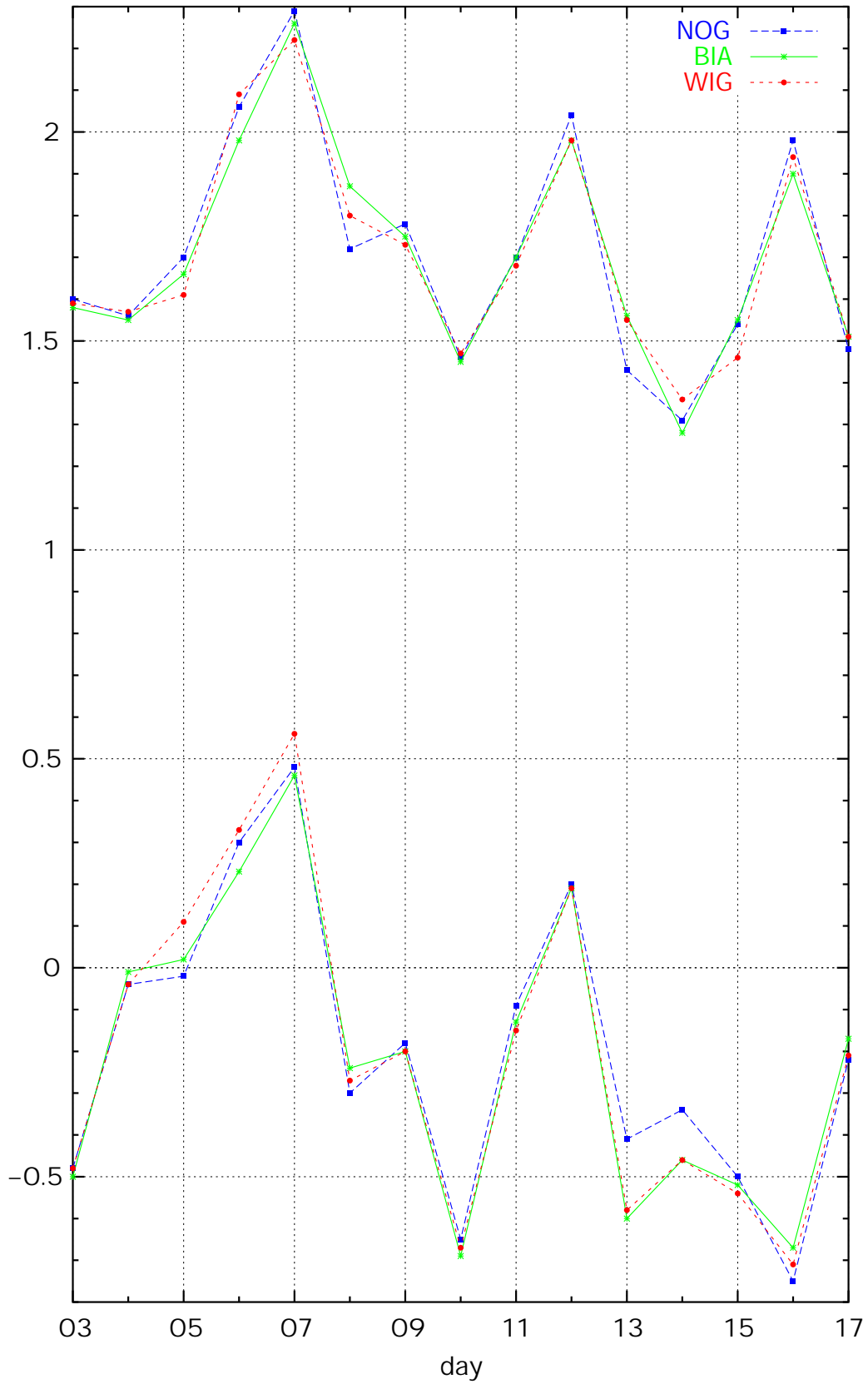
Figure 9: Daily obs-verification of 24 hours 850 hPa temperature forecasts.
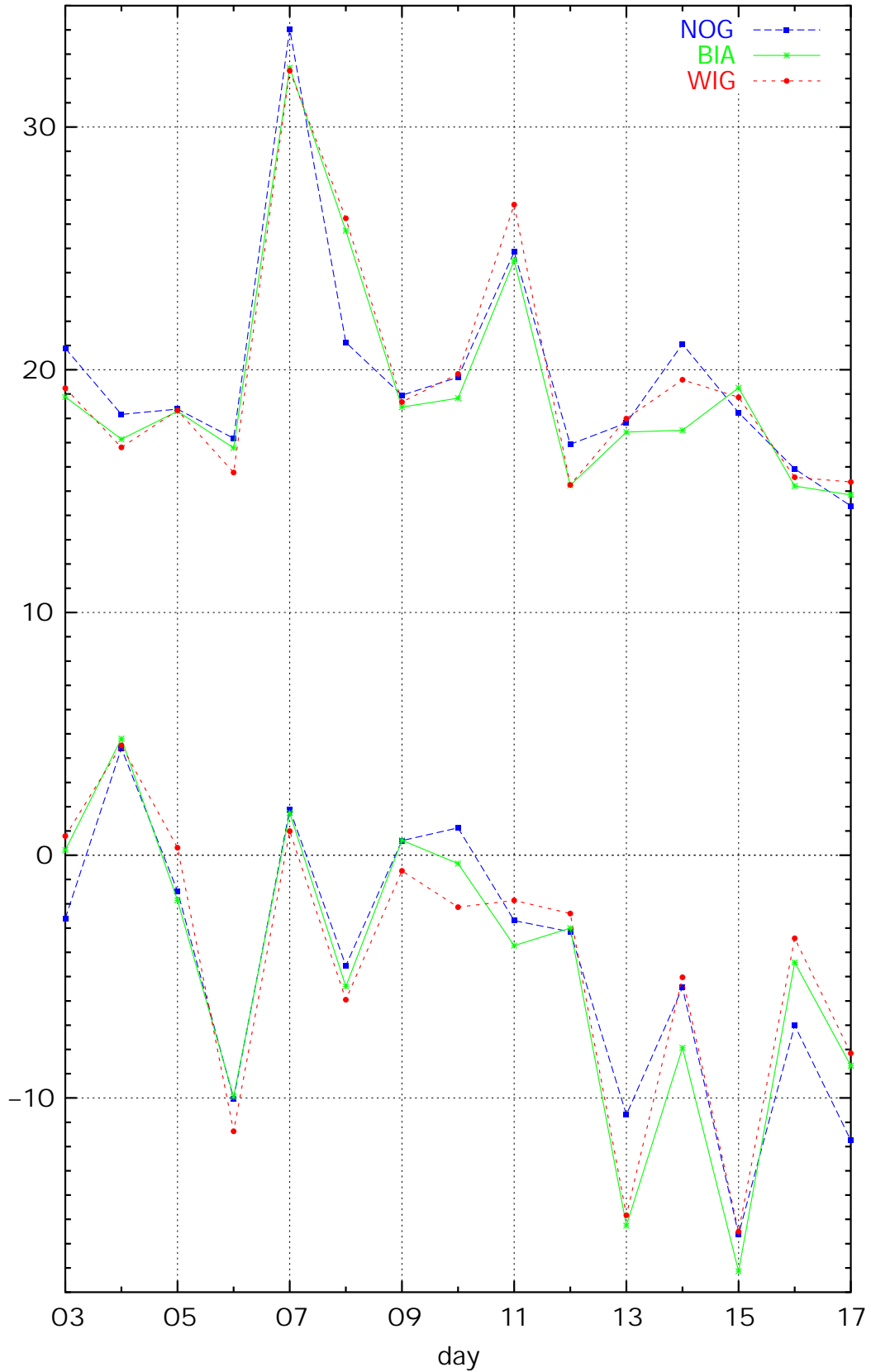
Figure 10: Daily obs-verification of 24 hours 500 hPa geopotential height forecasts.
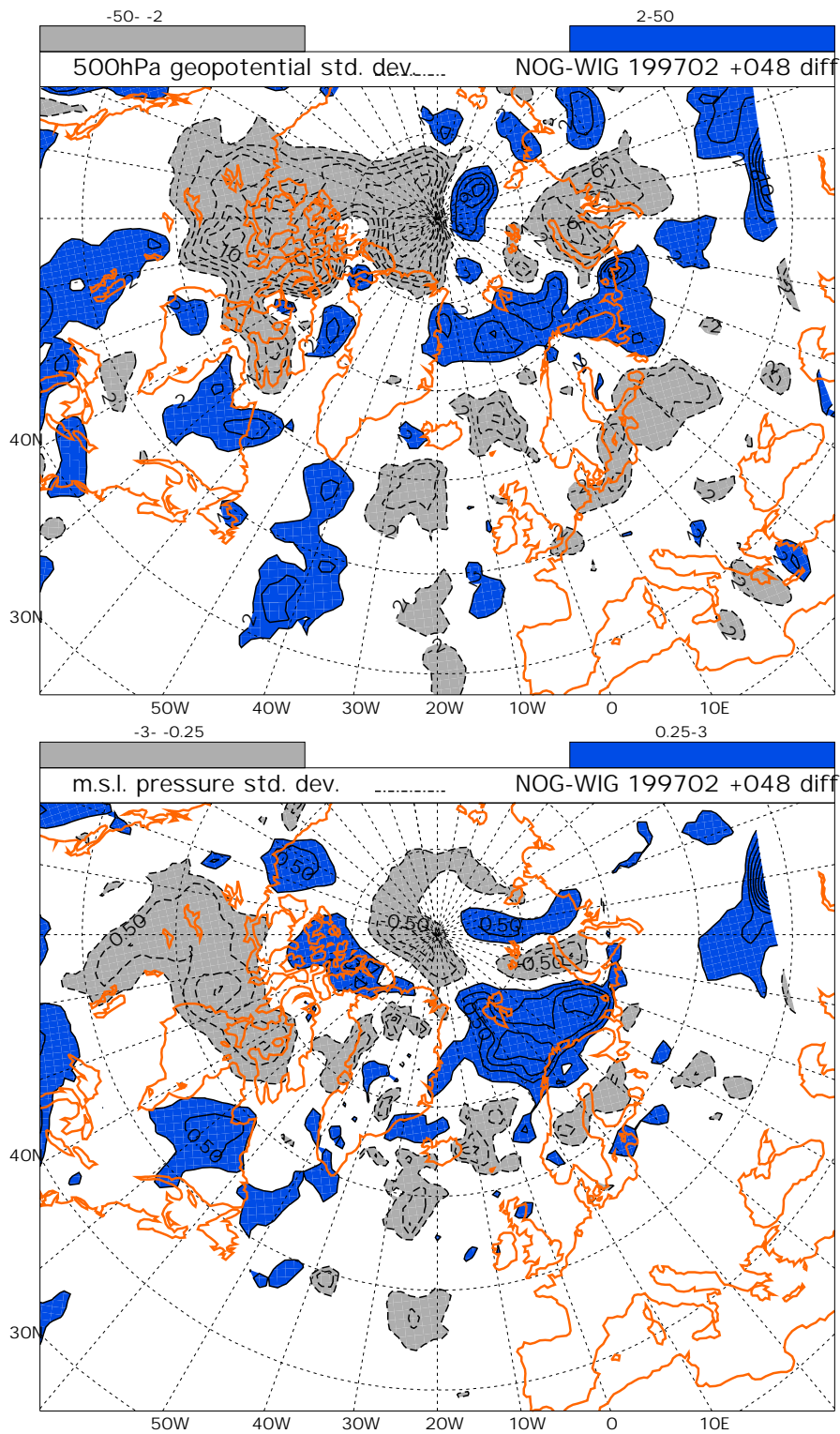
Figure 11: Difference of standard deviation between NOG ("control run", no GPS/MET data) and WIG (with GPS/MET data) for 48 h forecasts of 500 hPa geopotential height (upper) and mslp (lower) for the period. Full lines/blue shaded for areas where WIG has better and dashed lines/grey shaded for areas where NOG has better standard deviation. Contour lines are for every 2 m and 0.25 hPa, respectively.

17

system uses the radiosonde geopotentials. We could also take the temperature profiles produced by the same retrieval package (Syndergaard *et al.*, 2000). Healy (2000) has made a statistical analysis of GPS/MET temperature retrievals processed at DMI instead of geopotential as done here. He compared the GPS/MET data with temperature profiles derived from the Met Office unified model analyses. As we are in the process of replacing the OI based analysis by a variational data assimilation system, our future development may be towards using refractivity or bending angle profiles. We expect that the variational system will be able to extract temperature, humidity and surface pressure information from such data.

Acknowledgment

References

Daley, R. 1993. *Atmospheric Data Analysis*. Cambridge University Press. ISBN:0-521-45825-0.

Eyre, J. R. 1994. *Assimilation of radio occultation measurements into a numerical weather prediction system*. Technical Memorandum. ECMWF.

Gustafsson, N. 1990. Sensitivity of limited area model data assimilation to lateral boundary condition fields. *Tellus*, **42A**, 109–115.

Gustafsson, N. 1993. The HIRLAM 2 Final Report. *HIRLAM Technical Report*, **9**.

Healy, Sean B. 2000. *Validation and Statistical Analysis of the GPS/MET Data Processed at DMI*. CLIMAP Technical Note. UKMO. METOFFICE/CLIMAP/TN/02.

Høeg, P., Hauchecorne, A., Kirchengast, G., Syndergaard, S., Belloul, B., Leitinger, R. and Rothleitner, W. 1995. *Derivation of atmospheric properties using a radio occultation technique*. DMI Scientific Report 95-4. Danish Meteorological Institute.

Källén, E. 1996. *HIRLAM Documentation Manual. System 2.5*. Tech. rept. SMHI, Norrköbing, Sweden.

Lönnberg, P. and Shaw, D. (Eds.). 1987. *ECMWF Data Assimilation - Scientific Documentation. E*. ECMWF Research Manual 1, 2nd Revised Edition.

Lynch, Peter, Gustafsson, Nils, Sass, Bent Hansen and Cats, Gerard. 2000. Final Report of the HIRLAM 4 Project, 1997–1999. *HIRLAM 4 Final Report*.

Machenhauer, B. 1988. *HIRLAM final report*. HIRLAM Technical Report 5.

Sass, Bent Hansen, Nielsen, Niels W., Jørgensen, Jess U. and Amstrup, Bjarne. 1999. *The Operational HIRLAM System at DMI - October 1999 -*. DMI Technical Report 99-21. Danish Meteorological Institute.

Syndergaard, Stig, Sørensen, Martin B., Larsen, Georg B., Olsen, Laust, Grove-Rasmussen, Jakob and Høeg, Per. 2000. *The Ørsted–GPS radio occultation experiment: Data analysis and processing at DMI*. DMI Technical Report, Danish Meteorological Institute, to be published.

Undén, Per. 2000. HIRLAM Optimum Interpolation Upper Air Analysis. *Hirlam Scientific documentation*, to be published.

Vedel, Henrik. 2000. *Conversion of WGS84 geometric heights to NWP model HIRLAM geopotential heights*. Scientific Report 00-04. Danish Meteorological Institute.

Zou, X., Kuo, Y.-H. and Guo, Y.-R. 1994. Assimilation of atmospheric radio refractivity using a nonhydrostatic adjoint model. *Mon. Weather Rev.*, **123**, 2229–2249.

DANISH METEOROLOGICAL INSTITUTE

Scientific Reports

Scientific reports from the Danish Meteorological Institute cover a variety of geophysical fields, i.e. meteorology (including climatology), oceanography, subjects on air and sea pollution, geomagnetism, solar-terrestrial physics, and physics of the middle and upper atmosphere.

Reports in the series within the last five years:

No. 95-1
Peter Stauning and T.J. Rosenberg:
High-Latitude, day-time absorption spike events
1. morphology and occurrence statistics
Not published

No. 95-2
Niels Larsen: Modelling of changes in stratospheric ozone and other trace gases due to the emission changes : CEC Environment Program Contract No. EV5V-CT92-0079. Contribution to the final report

No. 95-3
Niels Larsen, Bjørn Knudsen, Paul Eriksen, Ib Steen Mikkelsen, Signe Bech Andersen and Torben Stockflet Jørgensen: Investigations of ozone, aerosols, and clouds in the arctic stratosphere : CEC Environment Program Contract No. EV5V-CT92-0074. Contribution to the final report

No. 95-4
Per Høeg and Stig Syndergaard: Study of the derivation of atmospheric properties using radio-occultation technique

No. 95-5
Xiao-Ding Yu, **Xiang-Yu Huang** and **Leif Laursen** and Erik Rasmussen: Application of the HIRLAM system in China: heavy rain forecast experiments in Yangtze River Region

No. 95-6
Bent Hansen Sass: A numerical forecasting system for the prediction of slippery roads

No. 95-7
Per Høeg: Proceeding of URSI International Conference, Working Group AFG1 Copenhagen, June 1995. Atmospheric research and applications using observations based on the GPS/GLONASS System
Not published

No. 95-8
Julie D. Pietrzak: A comparison of advection schemes for ocean modelling

No. 96-1
Poul Frich (co-ordinator), H. Alexandersson, J. Ashcroft, B. Dahlström, G.R. Demarée, A. Drebs, A.F.V. van Engelen, E.J. Førland, I. Hanssen-Bauer, R. Heino, T. Jónsson, K. Jonasson, L. Keegan, P.Ø. Nordli, **T. Schmith**, **P. Steffensen**, H. Tuomenvirta, O.E. Tveito: North Atlantic Climatological Dataset (NACD Version 1) - Final report

No. 96-2
Georg Kjærgaard Andreasen: Daily response of high-latitude current systems to solar wind variations: application of robust multiple regression. Methods on Godhavn magnetometer data

No. 96-3
Jacob Woge Nielsen, Karsten Bolding Kristensen, Lonny Hansen: Extreme sea level highs: a statistical tide gauge data study

No. 96-4
Jens Hesselbjerg Christensen, Ole Bøssing Christensen, Philippe Lopez, Erik van Meijgaard, Michael Botzet: The HIRLAM4 Regional Atmospheric Climate Model

No. 96-5
Xiang-Yu Huang: Horizontal diffusion and filtering in a mesoscale numerical weather prediction model

No. 96-6
Henrik Svensmark and Eigil Friis-Christensen: Variation of cosmic ray flux and global cloud coverage - a missing link in solar-climate relationships

No. 96-7
Jens Havskov Sørensen and Christian Ødum Jensen: A computer system for the management of epidemiological data and prediction of risk and economic consequences during outbreaks of foot-and-mouth disease. CEC AIR Programme. Contract No. AIR3 - CT92-0652

No. 96-8
Jens Havskov Sørensen: Quasi-automatic of input for LINCOM and RIMPUFF, and output conversi-

on. CEC AIR Programme. Contract No. AIR3 - CT92-0652

No. 96-9
Rashpal S. Gill and Hans H. Valeur:
Evaluation of the radarsat imagery for the operational mapping of sea ice around Greenland

No. 96-10
Jens Hesselbjerg Christensen, Bennert Machenhauer, Richard G. Jones, Christoph Schär, Paolo Michele Ruti, Manuel Castro and Guido Visconti:
Validation of present-day regional climate simulations over Europe: LAM simulations with observed boundary conditions

No. 96-11
Niels Larsen, Bjørn Knudsen, Paul Eriksen, Ib Steen Mikkelsen, Signe Bech Andersen and Torben Stockflet Jørgensen: European Stratospheric Monitoring Stations in the Artic: An European contribution to the Network for Detection of Stratospheric Change (NDSC): CEC Environment Programme Contract EV5V-CT93-0333: DMI contribution to the final report

No. 96-12
Niels Larsen: Effects of heterogeneous chemistry on the composition of the stratosphere: CEC Environment Programme Contract EV5V-CT93-0349: DMI contribution to the final report

No. 97-1
E. Friis Christensen og C. Skøtt: Contributions from the International Science Team. The Ørsted Mission - a pre-launch compendium

No. 97-2
Alix Rasmussen, Sissi Kiilsholm, Jens Havskov Sørensen, Ib Steen Mikkelsen: Analysis of tropospheric ozone measurements in Greenland: Contract No. EV5V-CT93-0318 (DG 12 DTEE): DMI's contribution to CEC Final Report Arctic Trophospheric Ozone Chemistry ARCTOC

No. 97-3
Peter Thejll: A search for effects of external events on terrestrial atmospheric pressure: cosmic rays

No. 97-4
Peter Thejll: A search for effects of external events on terrestrial atmospheric pressure: sector boundary crossings

No. 97-5
Knud Lassen: Twentieth century retreat of sea-ice in the Greenland Sea

No. 98-1
Niels Woetman Nielsen, Bjarne Amstrup, Jess U. Jørgensen:
HIRLAM 2.5 parallel tests at DMI: sensitivity to type of schemes for turbulence, moist processes and advection

No. 98-2
Per Høeg, Georg Bergeton Larsen, Hans-Henrik Benzon, Stig Syndergaard, Mette Dahl Mortensen: The GPSOS project
Algorithm functional design and analysis of ionosphere, stratosphere and troposphere observations

No. 98-3
Mette Dahl Mortensen, Per Høeg:
Satellite atmosphere profiling retrieval in a nonlinear troposphere
Previously entitled: Limitations induced by Multipath

No. 98-4
Mette Dahl Mortensen, Per Høeg:
Resolution properties in atmospheric profiling with GPS
No. 98-5
R.S. Gill and M. K. Rosengren
Evaluation of the Radarsat imagery for the operational mapping of sea ice around Greenland in 1997

No. 98-6
R.S. Gill, H.H. Valeur, P. Nielsen and K.Q. Hansen: Using ERS SAR images in the operational mapping of sea ice in the Greenland waters: final report for ESA-ESRIN's: pilot projekt no. PP2.PP2.DK2 and 2nd announcement of opportunity for the exploitation of ERS data projekt No. AO2..DK 102

No. 98-7
Per Høeg et al.: GPS Atmosphere profiling methods and error assessments

No. 98-8
H. Svensmark, N. Woetmann Nielsen and A.M. Sempreviva: Large scale soft and hard turbulent states of the atmosphere

No. 98-9
Philippe Lopez, Eigil Kaas and Annette Guldberg: The full particle-in-cell advection scheme in spherical geometry

No. 98-10
H. Svensmark: Influence of cosmic rays on earth's climate

No. 00-08

A.L. Morozova: Solar activity and Earth's weather. Effect of the forced atmospheric transparency changes on the troposphere temperature profile studied with atmospheric models

No. 00-09

Niels Larsen, Bjørn M. Knudsen, Michael Gauss, Giovanni Pitari: Effects from high-speed civil traffic aircraft emissions on polar stratospheric clouds

No. 00-10

Søren Andersen: Evaluation of SSM/I sea ice algorithms for use in the SAF on ocean and sea ice, July 2000
(In Press)

No. 00-11

Claus Petersen, Niels Woetmann Nielsen: Diagnosis of visibility in DMI-HIRLAM

No. 00-12

Erik Buch: A monograph on the physical oceanography of the Greenland waters
(In Press)